

## Spectroscopic Investigations of Intermolecular Interactions in Supercritical Fluids

M. A. KANE, S. N. DANIEL, E. D. NIEMEYER, F. V. BRIGHT

### 5.1 Introduction

Solvent choice is amongst the most important factors governing the efficiency, selectivity, and outcome of a chemical reaction, extraction, or separation. However, as a result of recent environmental legislation, the use of several common organic and especially chlorinated liquid solvents has been limited or even banned [1]. For this reason, researchers have begun intensive work to develop and exploit more “environmentally-friendly” or “green” solvents. At the forefront of this research has been the development of supercritical fluid technologies as an alternative to hazardous solvents currently in use [1–6].

When a pure substance is raised above its critical point (defined by its characteristic critical temperature ( $T_c$ ) and pressure ( $P_c$ )), the liquid and gas phases coalesce into a single phase, known as a supercritical fluid (Table 5.1). Once in the supercritical state, the properties of the fluid can be tuned continuously by simply adjusting the system temperature and/or pressure. Figure 5.1 illustrates the effects of system pressure and temperature on the bulk density and dielectric constant of supercritical  $\text{CO}_2$  ( $\text{scCO}_2$ ) at reduced temperatures ( $T_r = T_{\text{exp}}/T_c$ ) of 1.01 and 1.10. Examination of these isotherms shows that near the critical temperature, small changes in system pressure can lead to significant changes in the bulk fluid density. However, as one increases the system temperature ( $T_r > 1.00$ ) and moves further from the system critical point, one sees that the changes in density are not nearly as sensitive to pressure changes (Fig. 5.1 B, C).

**Table 5.1.** Critical data for several common supercritical fluids

Fluid	Critical Pressure (bar)	Critical Temperature (K)	Critical Density (g/ml)
$\text{CO}_2$	74	304	0.472
$\text{C}_2\text{H}_6$	49	306	0.204
$\text{C}_2\text{H}_4$	50	282	0.214
$\text{CF}_3\text{H}$	49	300	0.506
$\text{CF}_3\text{Cl}$	39	302	0.585
Xe	58	290	1.096
$\text{H}_2\text{O}$	221	648	0.281
$\text{N}_2\text{O}$	72	310	0.445

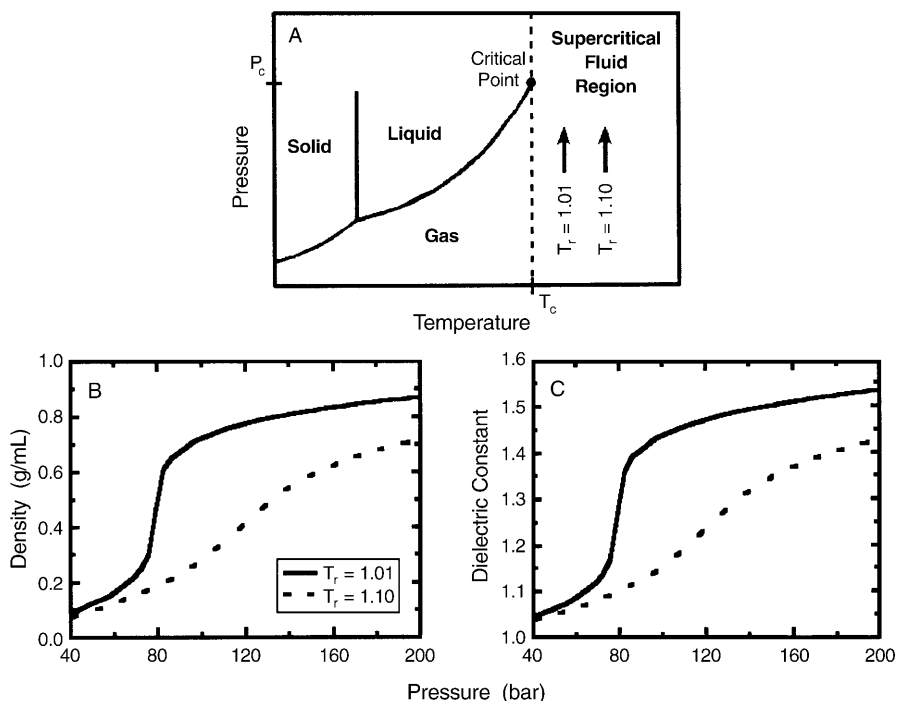


**Fig. 5.1 a–c.** Tunability of a supercritical fluid: **a** generic phase diagram for a pure substance; **b** density; **c** dielectric constant isotherms as a function of pressure for supercritical  $\text{CO}_2$  at  $T_r = 1.01$  and  $1.10$

One should also note that other physicochemical properties (e.g., refractive index, viscosity, diffusion coefficient), which scale with density, are also tunable with pressure and temperature. Thus, a supercritical fluid can be adjusted continuously between gas- and liquid-like properties without physically changing the solvent. Supercritical fluids also possess liquid-like solvation properties and have more gas-like diffusivities which can lead to higher mass transport rates in comparison to normal liquids. For these reasons, the uses of supercritical fluids continues to grow [1–6].

To date, the most commonly used supercritical fluids have been  $\text{CO}_2$  and  $\text{H}_2\text{O}$ . Carbon dioxide is inexpensive, non-toxic, nonflammable, and it has relatively mild critical parameters (Table 5.1). Supercritical  $\text{CO}_2$  has been used for the decaffeination of tea and coffee, the extraction of hops, spices, and flavorings, the extraction of pharmaceuticals from seeds and barks, to harden and strengthen Portland cement and building materials, and even as an alternative to perchloroethylene in the commercial dry cleaning process. Supercritical water (SCW) has attracted substantial interest because of its potential for hazardous waste disposal. Moreover, when water is raised above its critical point (Table 5.1), environmentally harmful organics can be rapidly and efficiently oxidized to benign compounds such as  $\text{CO}_2$ ,  $\text{H}_2\text{O}$ , and simple inorganic acids and salts. Cur-

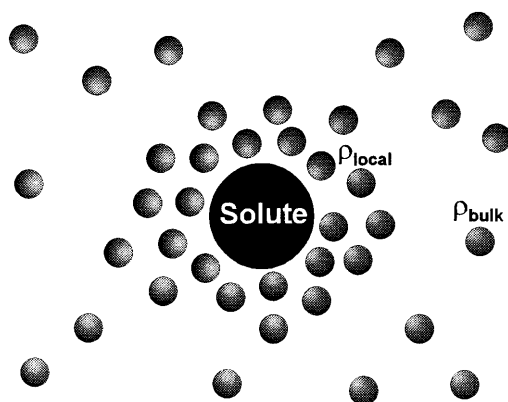


**Fig. 5.2.** A depiction of the solute-fluid density augmentation process with an increase in local density ( $\rho_{local}$ ) surrounding the solute compared to the bulk fluid density ( $\rho_{bulk}$ )

rently, there are several commercial waste disposal plants in operation in the US and Europe based on SCW wet oxidation technology. Supercritical water has also been used for the destruction of chemical arms and even of used automobile tires.

One of the most interesting phenomena observed in supercritical fluid systems is an apparent increase in the local fluid density, relative to the bulk density, surrounding a dissolved solute when the system is near the mixture critical point [7–10]. This increase in fluid density has been termed “solute-fluid clustering”, “molecular charisma”, or “local density augmentation.” A simplified depiction of the solute-fluid clustering process is shown in Fig. 5.2, with an increased local fluid density ( $\rho_{local}$ ) surrounding the solute compared to the lower bulk fluid density ( $\rho_{bulk}$ ). The solute-fluid clusters observed in supercritical fluids are *dynamic* in nature, constantly exchanging fluid molecules with the bulk fluid on a sub-picosecond time scale [11]. This augmentation phenomena is thought to influence a wide variety of processes including reaction rates and outcome, solute conformational equilibria, and extractions.

The remainder of this chapter will highlight several of the more varied applications of UV-Vis absorbance spectroscopy, fluorescence spectroscopy, and laser flash photolysis as they have been applied to the study of solute-fluid interactions within supercritical fluid systems. The reader should also realize that there is an extensive literature using, for example, infrared absorbance, Raman scattering, NMR, XAFS, and thermal optical methods that are intentionally not discussed in this chapter.

## 5.2 Instrumentation

It is well-known that certain chromophores/dyes exhibit features that are a strong function of the physicochemical properties of their surroundings [12]. As a result, one can use these sorts of chromophores as solute probes of *their* local

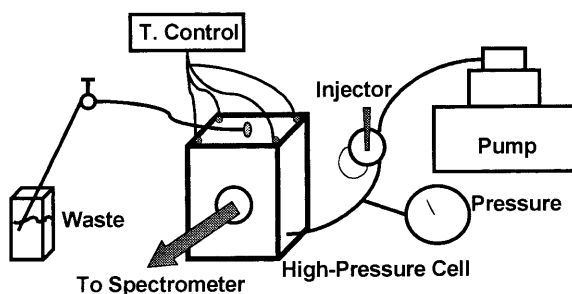


**Fig. 5.3.** Simplified schematic for a typical spectroscopy set-up for studying supercritical fluids

microenvironment. In this context techniques like absorbance and emission spectroscopy are almost ideal for addressing question about the local microenvironment surrounding a solute dissolved in a supercritical fluid. These techniques are also attractive because they allow one to assess the local microenvironment surrounding a solute, if the solute absorbs and/or emits, under conditions when the solute concentration is reasonably low. In this way one can minimize solute-solute interactions and focus exclusively on solute-fluid/solvent interactions.

To get a handle on the local microenvironment surrounding a solute dissolved in a supercritical fluid, one needs several pieces of equipment (Fig. 5.3). First, one needs a spectrometer. A spectrometer can range from a simple UV-Vis absorbance spectrophotometer up to a sophisticated time-resolved laser system. One needs a high-pressure optical cell to house the fluid. The high-pressure cell body is often made of stainless steel or some other suitable material (e.g., titanium). The choice of the cell material depends on the corrosive tendencies of the fluid itself and the temperature range to be studied. One also requires optical ports that will allow one to bring the electromagnetic radiation into and out of the fluid. In the UV/visible region, one might seal windows (quartz or sapphire) directly into the cell body or one might use optical fibers mounted within the cell body. Again, some care must be exercised in selecting the optical port materials depending on the sealing method that one intends to use (e.g., Teflon O-rings, Au seals), the temperature and pressure range of the experiments, and the corrosive nature of the fluid. A careful look at Fig. 5.2 shows that it is also important to control accurately and precisely *and know* the actual pressure and temperature within the high-pressure cell. A pump can serve to generate the pressure, a precision gauge is used to monitor the pressure within the high-pressure cell, and cartridge heaters are often used in concert with a thermocouple feed back system to control the cell/fluid temperature.

### 5.3 Sample Preparation and Precautions

There are several challenges associated with performing good spectroscopic measurements of solutes dissolved in supercritical fluids. Foremost amongst these issues is to ensure that the solute is actually dissolved completely in the fluid and not adsorbed to the interior cell walls or the optical ports. This challenge can be met by working at solute concentrations in the low micromolar range and by taking special care to look for and minimize signs of solute adsorption and/or aggregation. Unanticipated shifts in the spectral profiles with changes in fluid density, beyond continuum model predictions, are always good indicators of adsorbed species and/or aggregates, but these must always be decoupled from the intrinsic shifts induced by changes in the physicochemical properties of the fluid with changes in fluid density. A low micromolar solute concentration range also sets practical limits on the types of probes/solutes that one can effectively study. An ideal solute is one with: (1) a reasonably high *combination* of solubility in the fluid of choice over the density range in question, high molar extinction coefficient, and high fluorescence quantum yield and (2) a spectroscopically accessible signature (e.g., absorbance or emission spectrum, lifetime) that is strongly dependent on the physicochemical properties of the solvent. Examples of the more common solutes used for studying supercritical fluids include pyrene ( $I_1/I_3$  band ratio depends on the solvent), DMABN (undergoes twisted-intramolecular charge transfer to an extent that depends on the solvent properties), or *N,N'*-bis-(2,5-*tert*-butylphenyl)-3,4,9,10-perylenecarboxodiimide (rotational reorientation dynamics depend on the solvent microviscosity).

In our laboratory we always make sure the solutions are thoroughly mixed and we check for adsorption or aggregation by recording the static electronic absorbance spectra in a given fluid as a function of fluid density. In general, an absorbance profile that remains more or less constant (save for the shifts induced by changes in the fluid's orientational polarizability caused by changes in fluid density with changes in pressure) in magnitude is indicative of a fully dissolved solute. In questionable situations, we run a series of control experiments over a range of solute concentrations.

### 5.4 Selected Applications

The electronic absorbance and emission characteristics of a solute can be used to provide information on the local environment surrounding the molecule in its ground and excited state [12]. For this reason, absorbance and fluorescence studies have been one of the most popular methods to quantify solvation phenomena in supercritical fluids. For example, solvatochromic shifts in the absorbance and fluorescence spectra of solutes dissolved in a variety of supercritical fluid systems have been used extensively to quantify solute-fluid interactions. Time-resolved measurements have also been used to provide insight into solvation in supercritical fluids.

Fluorescence-based measurements are particularly attractive because the emission process contains a wealth of information that is related to the fluorophore (i.e., the solute) *and* its surroundings. Specifically, one can conveniently divide fluorescence techniques into two forms: static and dynamic. These can in turn be divided still further into subcategories with particular features:

### *Static*

#### Intensity

- Concentration of species
- Quenching of species (accessibility, conformational changes, kinetics of change)

#### Spectral

- Information on the local environment about the fluorophore (e.g., polarity, pH).
- Distances between sites via energy transfer techniques

#### Polarization/Anisotropy

- Average size of a rotationally reorienting species
- Mobility or motional restriction

### *Dynamic*

#### Excited-State Decay Kinetics

- Resolve static emission into the contribution from the individual emissive centers
- Study ultrafast kinetic processes (e.g., solvation)
- Unravel excited-state decay kinetics
- Elucidate origin of quenching processes
- Study exchange processes and heterogeneity (e.g., continuous lifetime distributions)

#### Excited-State Decay of Anisotropy

- Detailed reorientational dynamics of non-spherical rotors (e.g., diffusion kinetics)
- Overall shape of the rotating body
- Discrimination between local and global motions in a complex system

It is common for chemists and engineers to add a small amount (1–10 mol%) of a cosolvent (e.g., an alcohol) to  $\text{scCO}_2$  to improve extractions and increase solute loadings. Although this is a common practice, there is a limited amount of information on exactly how the cosolvent, fluid, and solute interact with one another. By using the  $n \rightarrow \pi^*$  absorbance shift of benzophenone, Eckert and co-workers [13] recently investigated the behavior of benzophenone dissolved in binary supercritical solutions composed of  $\text{C}_2\text{H}_6$  and a large variety of cosolvents. Because the benzophenone  $n \rightarrow \pi^*$  transition is sensitive to its local solvent environment, increases in local solvent dipolarity or specific solute-fluid interactions (i.e., hydrogen bonding) result in a blue shift of the  $n \rightarrow \pi^*$  absorbance. By using supercritical  $\text{C}_2\text{H}_6$  the authors were able to eliminate any possible

specific interactions with the benzophenone carbonyl and the fluid. The cosolvents that were chosen had hydrogen bonding abilities with the benzophenone. The authors found a maximum in the benzophenone  $n \rightarrow \pi^*$  shift occurred when they used the cosolvent 2,2,2-trifluoroethanol (TFE) and this shift was density independent at higher TFE concentrations. Upon examination of other cosolvents, with a lesser ability to hydrogen bond to benzophenone, the authors concluded that hydrogen bonding is the primary reason for changes in the  $n \rightarrow \pi^*$  absorbance shift within the supercritical  $C_2H_6$ /cosolvent/benzophenone system.

A chemical-physical model was developed to predict benzophenone  $n \rightarrow \pi^*$  shifts in the TFE/ $C_2H_6$  system. This model was based on the benzophenone  $n \rightarrow \pi^*$  shifts in liquids, and it assumes that the shifts observed in liquids and supercritical fluids arises from similar changes in local solvent dipolarity. The model was used to predict the maximum benzophenone  $n \rightarrow \pi^*$  shift as a function of  $C_2H_6$  density. The model under-predicted the experimental benzophenone  $n \rightarrow \pi^*$  shift at lower fluid densities and over-predicted the shift at higher fluid densities. This particular result was explained in terms of the model's inability to account for changes in local density and local cosolvent composition enhancements surrounding the benzophenone molecule in proximity to the fluid critical point. Additional integral equation analysis showed that, while this model assumed that the coordination number surrounding the benzophenone remains constant as a function of fluid density, the coordination number actually varies near the mixture critical point.

Schulte and Kauffman have exploited the fluorescence from twisted intramolecular charge transfer (TICT) molecules to quantify changes in the local solvent permittivity in a binary supercritical mixture composed of  $CO_2$  and ethanol. A TICT compound contains both an electron donor and electron acceptor group which must twist in the excited state for charge transfer to occur [14, 15]. TICT compounds are strongly solvatochromic and can exist as two isomers, either a locally excited (LE) or charge transfer (CT) configuration. If the TICT molecule is dissolved in a dipolar solvent, after electronic excitation it may twist to form the CT complex which has a much larger dipole moment and is therefore stabilized in the polar solvent. The CT emission band is strongly red shifted with respect to the LE band and its fluorescence quantum yield is strongly dependent on the solvent dipolarity. Due to their strongly solvatochromic characteristics, TICT compounds have been very popular for use in quantifying solvation in supercritical fluids. Schulte and Kauffman used bis(4,4'-aminophenyl)sulfone (APS) [14] and bis(4,4'-dimethylaminophenyl)sulfone (DMAPS) [15] to probe changes in local permittivity in ethanol-modified  $CO_2$  systems. Interestingly, although these compounds are structurally similar, APS is only soluble in ethanol-modified  $CO_2$  while DMAPS is soluble in either neat or ethanol-modified  $CO_2$ .

Comparison of LE and CT spectral shifts and intensities were made between APS in a 5 mol% mixture of ethanol in  $CO_2$  and APS dissolved in liquid  $n$ -alcohols. The authors found that in the low density fluid region, APS exists in an environment that is similar in permittivity to liquid  $n$ -butanol, but as the fluid pressure is increased ( $>124$  bar) the permittivity becomes more similar to liquid

*n*-octanol. Additionally, ratios of the CT to LE quantum yields were used to determine local solvent permittivity. Experimentally determined permittivities were compared to the empirically calculated bulk permittivities for the ethanol/CO<sub>2</sub> system. From this comparison, the authors showed that, in proximity to the fluid critical density, the permittivity was 8–10 times greater than the bulk permittivity. These results were discussed in terms of preferential solvation of the alcohol cosolvent surrounding the solute near the fluid mixture critical point.

When DMAPS was dissolved in neat CO<sub>2</sub>, changes in the fluid pressure resulted in no detectable spectral shifts, indicating that the spectral shifts noted above are a result of changes in the local solvent environment/composition and are not pressure induced. The authors also noted that the DMAPS emission intensity was much higher in the ethanol-modified CO<sub>2</sub> than in neat CO<sub>2</sub> due to the increased DMAPS solubility. As observed for APS in ethanol-modified CO<sub>2</sub>, in order for local permittivities to agree with the bulk ethanol/CO<sub>2</sub> permittivities, a local solvent enrichment factor, indicative of cosolvent-fluid compositional augmentation, was needed to describe the data.

The local microenvironment surrounding pyrene molecules perturbs the p-electronic orbitals via Herzberg-Teller symmetry distortions and this affects the  $B_u^2$  and  $B_u^1$  interstate coupling efficiency. This vibronic coupling enhances the otherwise forbidden transition from the  $B_u^2$  excited state to the ground state, resulting in an  $I_1$  emission band intensity (normally appearing near 373 nm) and excited-state singlet fluorescence lifetimes that are strongly dependent on the physicochemical properties of the local environment. The environmental sensitivity is manifest by changes in the pyrene  $I_1/I_3$  band ratio and the excited-state fluorescence lifetime. Specifically, the pyrene  $I_1/I_3$  increases with increasing solvent dipolarity. Thus, by measuring the pyrene  $I_1/I_3$  ratio as a function of bulk fluid density and/or composition, insight can be gained into the local environment surrounding the pyrene within the supercritical fluid mixtures.

Brennecke and co-workers [16] have recently used the steady-state fluorescence emission of dilute pyrene solutions to determine the nature of solvation in sub- and supercritical fluid mixtures of CO<sub>2</sub> and CF<sub>3</sub>H as a function of fluid density. Mixtures of CO<sub>2</sub> and CF<sub>3</sub>H were chosen for this study because they have similar critical points (see Table 5.1) and their mixtures maintain highly compressible regions similar to neat supercritical fluids. These experiments showed that the pyrene  $I_1/I_3$  always increased with fluid density at all temperatures and with all fluids (neat and mixtures). In addition,  $I_1/I_3$  is linear with bulk fluid density in the higher density region (similar to pyrene in other fluids) [17]; however, there were substantial nonlinearities in  $I_1/I_3$  in the density region near and below the critical density. This deviation in the low density region was used to estimate the local fluid composition/density surrounding the pyrene in the neat fluids as well as the fluid mixtures. The calculated  $\rho_{\text{local}}/\rho_{\text{bulk}}$  (a measure of the extent of density augmentation surrounding the pyrene molecules) for all systems was found to be smaller overall at higher temperatures and to reach a maximum well below the bulk critical density. The authors estimated that the solvent strength for CO<sub>2</sub> in a CF<sub>3</sub>H rich mixture was nearly the same in the intermediate density region as pure CF<sub>3</sub>H, indicating an exclusion of CO<sub>2</sub> in the



pyrene solvation sphere and, hence, preferential solvation of the pyrene by the  $\text{CF}_3\text{H}$ . For the mixture in which  $\text{CO}_2$  predominated, analysis of solvent strength also indicated preferential solvation by  $\text{CF}_3\text{H}$  in the high density region. However, in the intermediate pressure range, the solvation strength was more similar to a  $\text{CO}_2$ -like environment, indicating a depletion of  $\text{CF}_3\text{H}$  before returning to a more  $\text{CF}_3\text{H}$  rich environment at lower bulk fluid densities.

Fluorescence quantum yields and excited-state lifetimes of a model solute (9-cyanoanthracene, 9CA) dissolved in supercritical  $\text{C}_2\text{H}_6$ ,  $\text{CO}_2$ , and  $\text{CF}_3\text{H}$  over a wide density range were used by Rice et al. [18] to quantify energy dissipation processes within solute-fluid “clusters.” The fluorescence quantum yield ( $\Phi$ ) of a solute is related to its excited-state fluorescence lifetime ( $\tau$ ) and its radiative decay rate ( $k_r$ ) by the following equation:

$$k_r = \Phi/\tau \quad (5.1)$$

where the radiative decay rate ( $k_r$ ) is related to the non-radiative decay rate ( $k_{nr}$  where  $k_{nr} = 1/\tau - k_r$ ). Thus, by determining the fluorophore quantum yield and excited-state fluorescence lifetime, one can access directly how the solute dissipates energy to the solvent bath.

The 9CA quantum yield is effectively unity in liquids. However, the experimentally determined 9CA quantum yields in supercritical  $\text{C}_2\text{H}_6$ ,  $\text{CO}_2$ , and  $\text{CF}_3\text{H}$  are significantly less than unity at low fluid densities before approaching unity in the high density liquid-like region. Rice et al. also found that  $k_r$  and  $k_{nr}$  were strongly density dependent, with the nonradiative rate dominating in the low density region and the radiative rate dominating in the high density region. The Strickler-Berg relationship provides a theoretical construct between the measured fluorophore radiative decay rate and the solvent physical properties:

$$k_r = 2900 n^2 \nu_0^2 \int \epsilon d\nu \quad (5.2)$$

In this expression  $n$  denotes the solvent refractive index,  $\nu_0$  is the peak frequency of the fluorophore absorption spectrum, and  $\int \epsilon d\nu$  is the integrated area under a curve of the molar extinction coefficient as a function of wavenumber. In liquids the 9CA radiative rate is well described by Eq. (5.2). Rice et al. found that significant deviations from the Strickler-Berg expression occurred in the low density regions for each of the fluids and that corrections accounting for the change in refractive index and the change in absorbance shift for 9CA could not account fully for the observed deviations. The authors proposed that changes in the 9CA molar absorptivity in the low density region below the critical point is partially responsible for the deviation from the Strickler-Berg equation. The authors also argued that the dependence of  $k_{nr}$  and  $k_r$  on bulk fluid density was ultimately a result of local solute-fluid solvation and density-dependent, fluid-induced changes in the Franck-Condon factors between the 9CA  $S_1$  singlet state and a nearby triplet state  $T_2$ .

Anderton and Kauffman used fluorescence depolarization measurements to examine the effects of solute functionality on fluid density augmentation in supercritical  $\text{CO}_2$  [19]. By using two fluorescent solutes that have structures differ-

ing primarily by only a hydroxyl moiety (*trans*, *trans*-1,4-diphenylbutadiene (DPB) and *trans*-4-(hydroxymethyl)stilbene (HMS)) the authors were able to determine how a single functional group affected the degree of local density augmentation in CO<sub>2</sub>. The authors found that, over a CO<sub>2</sub> density range from 0.3 to 0.8 g/ml, DPB exhibits a slight increase in rotational reorientation time ( $\phi$ ) as a function of fluid density. In contrast, HMS (the hydroxylated analog) exhibits a much larger increase in its rotational reorientation time as the fluid density increased. Anderton and Kauffman proposed a model to interpret this rotational data based on a radial distribution function formalism in which the local solvent density,  $\rho_{1,2}^l(r)$ , surrounding a solute is related to the bulk fluid density ( $\rho$ ) and pair distribution function,  $g_{1,2}(r)$ , (where  $r$  is the distance between solvent, molecule 1, and solute, molecule 2):

$$\rho_{1,2}^l(r) = [1 + F(g_{1,2}(r))] \quad (5.3)$$

and  $F(g_{1,2}(r))$  is an integral equation in  $g_{1,2}(r)$  over the spatial coordinates that describe the local solvent density surrounding the solute molecule. By modeling the boundary conditions for the system as a function of the local fluid density, the solvent density augmentation parameter,  $F(g_{1,2}(r))$ , was used to predict the rotational reorientation times which were in turn used with the experimentally recovered solute rotational reorientation times to estimate the extent of solute-fluid density augmentation. In this formalism, when  $F(g_{1,2}(r)) = 0$ , the local density equals the bulk fluid density (i.e., no solute-fluid density augmentation is occurring). In contrast, when  $F(g_{1,2}(r)) = 1$  the local fluid density is twice the bulk density. The authors found that the local fluid density surrounding HMS was approximately 40% greater than that surrounding DPB, but there appeared to be no bulk density dependence in the degree of local density augmentation. The differences between HMS and DPB were explained in terms of an increase in degree of CO<sub>2</sub> local density augmentation surrounding the HMS hydroxyl moiety resulting from specific intermolecular interactions between CO<sub>2</sub> and HMS.

Heitz and Bright [20] used the Anderton and Kauffman model to explain the rotational reorientation of a large model solute (*N,N'*-bis(2,5-*tert*-butylphenyl)-3,4,9,10-perylenecarboxodiimide (BTBP)) in supercritical CO<sub>2</sub>, CF<sub>3</sub>H, and C<sub>2</sub>H<sub>6</sub>. The rotational reorientation time ( $\phi$ ) for BTBP in liquids was shown to follow simple hydrodynamic theory and obeyed the Debye-Stokes-Einstein (DSE) equation:

$$\phi = \eta V / RT \quad (5.4)$$

where  $\eta$  is the solvent viscosity,  $V$  is the volume of the reorienting species,  $R$  is the gas constant, and  $T$  is the absolute temperature. In supercritical fluids, the authors found that the BTBP measured rotational reorientation time deviated significantly from Debye-Stokes-Einstein predictions in the low density fluid region. At higher fluid densities/viscosities, the experimentally measured BTBP rotational reorientation times were well described by the DSE equation; however, at low fluid densities nearer the critical point, the BTBP rotational reorientation times were much higher than predicted. This was attributed to local den-

sity augmentation of the fluid about the BTBP which led to slower rotational reorientation times via either an increased reorienting species volume or an increased local viscosity surrounding the BTBP molecule compared to the bulk fluid. Using the Anderton and Kauffman model to determine the degree of local density augmentation surrounding the BTBP, the authors estimated that the extent of local density augmentation surrounding BTBP was approximately three times the bulk fluid density. Assuming that the deviation from DSE was a result of a larger rotating unit (i.e., BTBP + fluid molecules), the solute-fluid cluster size was estimated. The authors estimated that the BTBP-fluid cluster radius was approximately double the BTBP radius alone in  $\text{CF}_3\text{H}$  at the largest degree of density augmentation. Using the van der Waals volume for the fluid and the volume of the solute cluster, it was estimated that as many as three layers of fluid molecules were in the immediate solvation shell surrounding the BTBP in the low density region.

Although supercritical water shows tremendous promise for hazardous waste disposal (see above) there have been a limited number of fluorescence or absorbance spectroscopic studies to date on supercritical water. Most of the dearth of spectroscopic data arises from the fact that it is relatively difficult to work with and generate supercritical water. Johnston and co-workers have developed special optical cells and used absorbance spectroscopy [21] in tandem with steady-state and time-resolved fluorescence [22, 23] to characterize the acid-base behavior of a model solute in supercritical water. This work has focused on the behavior of  $\beta$ -naphthol, a fluorescent compound in which the lowest excited singlet state is significantly more acidic ( $pK_a^* = 2.5$ ) than its ground state ( $pK_a = 9.5$ ) in liquid water near ambient conditions. Initially, the equilibrium constant for the reaction between  $\beta$ -naphthol and the hydroxyl ion was studied using the solvatochromic shifts of the  $\beta$ -naphtholate anion. More recently, Johnston's team used time-resolved fluorescence measurements to quantify the excited-state deprotonation of  $\beta$ -naphthol in sub- and supercritical water solutions [22]. Although the proton transfer rate from  $\beta$ -naphthol to water follows Arrhenius behavior up to 353 K, the authors found that there were deviations from Arrhenius behavior above 383 K. On increasing the temperature to the critical point, the deviation from the Arrhenius model became much larger. This deviation was attributed to the unique properties of supercritical water that affected deprotonation at high temperatures in ways not well-described by extrapolation of the Arrhenius model. Most recently, Johnston's group extended this work to study excited-state proton transfer reactions from  $\beta$ -naphthol dissolved in supercritical water [23]. They determined that deprotonation of  $\beta$ -naphthol by acetate and borate anions in supercritical water leads to very small deviations from Arrhenius behavior. In contrast, deprotonation by ammonia or water leads to much greater deviations from the model. These results were explained in terms of the dependence of these reaction rates on changes in electric charge throughout the reaction where isocoulombic reactions differ little from Arrhenius behavior. The authors also showed that extrapolation of low temperature measurements to higher temperatures can approximate kinetic behavior well at high temperatures for the isocoulombic reactions of  $\beta$ -naphthol with acetate and borate anions.

## 5.5 Laser Flash Photolysis

Laser flash photolysis (LFP) and transient absorption measurements have been used for the quantification of energy transfer and diffusion-controlled reactions in supercritical fluids [24–31]. For example, Worrall and Wilkinson [24] have studied the rate of triplet-triplet energy transfer for the anthracene/azulene and benzophenone/naphthalene donor/acceptor systems and determined how the reaction rate is affected by cosolvent concentration in  $\text{scCO}_2$ . By first studying the effect of changing cosolvent ( $\text{CH}_3\text{CN}$  or  $n$ -hexane) on the anthracene/azulene system, the authors determined that the rate of energy transfer for this system was not affected by the cosolvent used. Further, by studying the rate of energy transfer for the benzophenone/naphthalene system in liquid  $n$ -hexane, the rate of energy transfer was shown to be statistically similar for both systems for a given mol fraction of  $n$ -hexane modifier. The authors also showed that above 0.5 mol fraction modifier the diffusion rates for all systems were nearly identical to those in the neat cosolvent. Rate constants for energy transfer were calculated for each of the systems, and from this, values for the probability of energy transfer ( $p$ ) was calculated. As the limit of zero mol fraction was approached, the value for the probability of energy transfer exceeded the value measured in neat modifier. These deviations at low mol fractions were explained by a model wherein the local concentration of modifier (and quencher) surrounding the solute was greater than the concentration in the bulk, possibly resulting in the greater energy transfer efficiency observed.

Brennecke and coworkers have done extensive work using laser flash photolysis to study diffusion-controlled reactions in supercritical fluids [25–29]. However, the authors have had to estimate the true solute diffusion coefficients in the supercritical fluid mixtures because there is significant deviation between the diffusion coefficients predicted by hydrodynamic theories and the available true values that have been measured in supercritical fluid solutions near and below the critical points. In one series of experiments, Brennecke and coworkers used the triplet-triplet annihilation of benzophenone ( $^3\text{BP}$ ) and self-termination of the benzyl radical to investigate how supercritical fluids might affect diffusion-controlled processes [25, 26]. The triplet-triplet annihilation of  $^3\text{BP}$  and the benzyl radical recombination reactions are bimolecular processes that are diffusion controlled in liquids. The triplet-triplet annihilation of  $^3\text{BP}$  exhibited clean second order decay kinetics in supercritical  $\text{CO}_2$ ,  $\text{CF}_3\text{H}$ , and in 1 mol%  $\text{CH}_3\text{CN}$ -modified  $\text{CO}_2$ . Further, there was no indication that addition of a cosolvent in any way slowed or impeded the diffusion-controlled reaction. The benzyl radical termination reaction also exhibited clean second order kinetics at the diffusion-controlled limit in supercritical  $\text{CO}_2$  and  $\text{C}_2\text{H}_6$  when spin statistical factors were taken into account. In addition, the photodecomposition of dibenzylketone (DBK) and subsequent decarbonylation of the phenylacetyl radical showed that the rate constants were approximately the same between the reaction in  $\text{CO}_2$ ,  $\text{C}_2\text{H}_6$ ,  $\text{CF}_3\text{H}$ , and  $\text{CH}_3\text{CN}$ -modified  $\text{CO}_2$ . All of this evidence combines to show that diffusion-controlled reactions, despite increases in local solvent density surrounding a solute near the critical point, exhibit no significant

change in reaction kinetics due to any local phenomena. That is, because these reactions occur at the diffusion-controlled limit in neat and/or cosolvent-modified fluids, there was no indication that solvent-solute or solute-solute interactions changed the reaction kinetics. In addition, adding small amounts of a cosolvent were shown to have no effect on the diffusion-controlled reaction rates.

## 5.6 Basic Picture Revealed by These Studies

Based on the results from a wide range of spectroscopic techniques, a clearer view of the molecular-level interactions occurring within these supercritical fluids has begun to emerge [32]. From initial work involving absorbance and fluorescence measurements of solvatochromic dyes in supercritical fluids, the solute-fluid density augmentation process has become better understood in simple fluid systems involving a single dissolved solute. It is known that an increase in local density with respect to the bulk occurs near the fluid critical point with a maximum in this local density occurring at around one-half the critical density. Moreover, the addition of a cosolvent has been shown to increase the local cosolvent composition surrounding a dissolved solute near the critical point which leads to preferential solvation of a solute by the cosolvent that can be controlled by adjusting the fluid pressure.

## 5.7 The Future

Although we have learned much about supercritical fluids over the past decade, we will continue to see new efforts to understand ever more complex, multi-component fluid systems. We can foresee three major areas where spectroscopy will impact supercritical fluid science and technology.

Several research groups have recently shown that one can form thermodynamically stable reverse micelles and microemulsions in  $\text{scCO}_2$  [33–37]. The most widely reported of these new micelle systems are those based on PFPE (perfluoropolyether ammonium carboxylate) surfactants [33, 38–40]. Over the past few years several key aspects of the PFPE/ $\text{scCO}_2$ / $\text{H}_2\text{O}$  system have been investigated, including their phase equilibria, water pool and micelle shape, and internal dynamics [38], the pH within an unbuffered PFPE water pool [39] and a means to control the water pool pH within PFPE micelles [40]. Several researchers have also shown that one can use the PFPE/ $\text{CO}_2$ / $\text{H}_2\text{O}$  system to perform inorganic [41] and organic [42, 43] reactions directly within the micelle water pool. Researchers have also used these micelles to prepare tailored, uniform CdS nanoparticles [44]. Finally, researchers have performed enzymatic reactions within micelles/microemulsions formed in liquid [45] and  $\text{scCO}_2$  [46]. We envisage questions on the behavior of proteins and the like within these microemulsions to be addressed by optical spectroscopic methods.

In solution, polymer behavior can be controlled by the choice of solvent, solution composition, or temperature. For example, the tail-tail segment dynamics of a polymer dissolved in a “good” solvent are significantly different to those of

the same polymer dissolved in a  $\theta$  or “bad” solvent. Given this, one can clearly control polymer dynamics, especially at the tail segments, by adjusting the solvent properties. DeSimone and his group have shown [47, 48] that one can perform homogeneous free radical polymerizations and the like by using environmentally friendly near- and supercritical  $\text{CO}_2$  as the reaction solvent. The results of these efforts have been remarkable and they demonstrate the tremendous potential of supercritical  $\text{CO}_2$  as a polymerization solvent [47, 48]. However, even though the promise and potential of polymerization reactions in supercritical  $\text{CO}_2$  are great, there have only been a limited number of reports [49–55] on the molecular-level events that dilute polymer solutions undergo within a supercritical fluid. It seems clear that spectroscopic measurements can be used to help elucidate polymer behavior within supercritical fluid systems.

The interactions between an enzyme and a supercritical fluid are of great interest to many researchers because the inherent tunability of the fluid continuous phase (Fig. 5.2) could provide a means to tune enzyme activity. In an effort to determine how a supercritical fluid affects the conformational changes of an enzyme, Ikushima et al. [56, 57] have used FTIR spectroscopy to determine the interactions between a model enzyme (*Candida cylindracea* (CCL)) and supercritical  $\text{CO}_2$ . The enzyme amide infrared absorption bands were used to provide information about the secondary protein structure. The authors determined that there was a decrease in  $\alpha$ -helical structure within the enzyme near the  $\text{CO}_2$  critical point. This result was related to the opening of the “lid” within the enzyme that exposed possible active sites for the biocatalysis reaction. Thus, near the  $\text{CO}_2$  critical point, these large conformational changes in the enzyme were likened to a “stereoselective machinery” capable of tuning the product enantiomeric excess. Again, this and other systems are amenable to spectroscopic investigation.

In summary, we envision fluorescence continuing to play an important role in the determination of fundamental processes of complex systems within supercritical fluid systems.

**Acknowledgements.** We thank the Division of Chemical Sciences, Office of Basic Energy Sciences, Office of Energy Research, United States Department of Energy (DEFGO290ER14143), and the American Chemical Society Analytical Division Fellowship (to EDN) sponsored by DuPont for support of our spectroscopic work in supercritical fluids.

## References

1. Via J, Taylor LT (1993) Solving process problems with supercritical-fluid extraction. *CHEMTECH* 23:38–44
2. Johnston KP, Penninger JML (1989) Supercritical fluid science and technology, vol 406. American Chemical Society, Washington, DC
3. Bruno TJ, Ely JF (1991) Supercritical fluid technology – reviews in modern theory and applications. CRC Press, Boca Raton, FL
4. Bright FV, McNally MEP (1992) Supercritical fluid technology – theoretical and applied approaches in analytical chemistry, vol 488. American Chemical Society, Washington, DC
5. Kiran E, Brennecke JF (1993) Supercritical fluid engineering science – fundamentals and applications, vol 514. American Chemical Society, Washington, DC



6. Jessop PG, Leitner W (1999) Chemical synthesis using supercritical fluids. Wiley-VCH, Germany
7. Kauffman JF (1996) Spectroscopy of solvent clustering in supercritical fluids. *Anal Chem* 68:248A–253A
8. Tucker SC, Madox MW (1998) The effect of solvent density inhomogeneities on solute dynamics in supercritical fluids: a theoretical perspective. *J Phys Chem B* 102:2437–2453
9. Kim S, Johnston KP (1987) Clustering in supercritical fluid mixtures. *AIChE J* 33: 1603–1611
10. Eckert CA, Knutson BL (1993) Molecular charisma in supercritical fluids. *Fluid Phase Equil* 83:93–100
11. Petsche IB, Debenedetti PG (1989) Solute-solvent interactions in infinitely dilute supercritical mixtures: a molecular dynamics investigation. *J Chem Phys* 91:7075–7084
12. Lakowicz JR (1999) Principles of fluorescence spectroscopy, 2nd edn. Kluwer, New York, NY
13. Knutson BL, Sherman SR, Bennet KL, Liotta CL, Eckert CA (1997) Benzophenone as a probe of local cosolvent effects in supercritical ethane. *Ind Eng Chem Res* 36:854–868
14. Schulte RD, Kauffman JF (1994) Solvation in mixed supercritical fluids – TICT spectra of bis(4,4'-aminophenyl) sulfone in ethanol/CO<sub>2</sub>. *J Phys Chem* 98:8793–8800
15. Schulte RD, Kauffman JF (1995) Fluorescence from the twisted intramolecular charge-transfer compound bis(4,4'-dimethylaminophenyl)sulfone in ethanol/CO<sub>2</sub> – a probe of local solvent composition. *Appl Spectrosc* 49:31–39
16. Zhang J, Lee LL, Brennecke JF (1995) Fluorescence spectroscopy and integral-equation studies of preferential solvation in supercritical-fluid mixtures. *J Phys Chem* 99: 9268–9277
17. Rice JK, Niemeyer ED, Dunbar RA, Bright, FV (1995) State-dependent solvation of pyrene in supercritical CO<sub>2</sub>. *J Am Chem Soc* 117:5832–5839
18. Rice JK, Niemeyer ED, Bright FV (1996) Solute-fluid coupling and energy dissipation in supercritical fluids: 9-cyanoanthracene in C<sub>2</sub>H<sub>6</sub>, CO<sub>2</sub>, and CF<sub>3</sub>H. *J Phys Chem* 100: 8499–8507
19. Anderton RM, Kauffman JF (1995) Rotational relaxation in the compressible region of CO<sub>2</sub> – evidence for solute-induced clustering in supercritical-fluid solutions. *J Phys Chem* 99:13,759–13,762
20. Heitz MP, Bright FV (1996) Probing the scale of local density augmentation in supercritical fluids: a picosecond rotational reorientation study. *J Phys Chem* 100:6889–6897
21. Bennett GE, Johnston KP (1994) UV-visible absorbency spectroscopy of organic probes in supercritical water. *J Phys Chem* 98:441–447
22. Green, S, Xiang T, Johnston JP, Fox MA (1995) Excited-state deprotonation of beta-naphthol in supercritical water. *J Phys Chem* 99:13,787–13,795
23. Ryan ET, Xiang T, Johnston KP, Fox MA (1996) Excited-state proton transfer reactions in subcritical and supercritical water. *J Phys Chem* 100:9395–9402
24. Worrall DR, Wilkinson F (1996) Photochemistry in modified supercritical carbon dioxide – effect of modifier concentration on diffusion probed by triplet-triplet energy transfer. *J Chem Soc Faraday Trans* 92:1467–1471
25. Roberts CB, Zhang J, Chateauneuf JE, Brennecke JF (1993) Diffusion-controlled reactions in supercritical CHF<sub>3</sub> and CO<sub>2</sub>/acetonitrile mixtures. *J Am Chem Soc* 115:9576–9582
26. Roberts CB, Zhang J, Brennecke JE, Chateauneuf, JE (1993) Laser flash-photolysis investigations of diffusion-controlled reactions in supercritical fluids. *J Phys Chem* 97: 5618– 5623
27. Roberts CB, Chateauneuf JE, Brennecke JF (1992) Unique pressure effects on the absolute kinetics of triplet benzophenone photoreduction in supercritical CO<sub>2</sub>. *J Am Chem Soc* 114:8455–8463
28. Roberts CB, Brennecke JF, Chateauneuf JE (1993) Spectral shifts in the triplet-triplet absorption-spectrum of anthracene in supercritical fluids. *J Chem Soc Chem Comm* 868–869
29. Roberts CB, Brennecke JF, Chateauneuf JE (1995) Solvation effects on reactions of triplet benzophenone in supercritical fluids. *AIChE J* 41:1306–1318

30. Ji Q, Eyring EM, vanEldick R, Johnston KP, Goates SR, Lee ML (1995) Laser flash-photolysis studies of metal-carbonyls in supercritical CO<sub>2</sub> and ethane. *J Phys Chem* 99: 13,461–13,466
31. Ji Q, Lloyd CR, Eyring EM, vanEldick R (1997) Probing the solvation properties of liquid versus supercritical fluids with laser flash photolysis of W(CO)<sub>6</sub> in the presence of 2,2'-bipyridine. *J Phys Chem A* 101:243–247
32. Brennecke JF, Chateaneuf JE (1999) Homogeneous organic reactions as mechanistic probes in supercritical fluids. *Chem Rev* 99:433–452
33. Johnston KP, Harrison KL, Clarke MJ, Howdle SM, Heitz MP, Bright FV, Carlier C, Randolph TW (1996) Water in carbon dioxide microemulsions: an environment for hydrophiles including proteins. *Science* 271:624–626
34. McClain JB, Betts DE, Canelas DA, Samulski ET, De Simone JM, Londono JD, Cochran HD, Wignall GD, Chillura-Martino D, Triolo R (1996) Design of nonionic surfactants for supercritical carbon dioxide. *Science* 274:2049–2052
35. Eastoe J, Cazelles BMH, Steytler DC, Holmes JD, Pitt AR, Wear TJ, Heenan RK (1997) Water-in-CO<sub>2</sub> microemulsions studied by small-angle neutron scattering. *Langmuir* 13:6980–6984
36. Ghenciu EG, Russell AJ, Beckman EJ, Steele L, Becker NT (1998) Solubilization of subtilisin in CO<sub>2</sub> using fluoroether-functional amphiphiles. *Biotechnol Bioengr* 58:572–580
37. Salaniwal S, Cui ST, Cummings PT, Cochran HD (1999) Self-assembly of reverse micelles in water/surfactant/carbon dioxide systems by molecular simulation. *Langmuir* 15: 5188–5192
38. Heitz MP, Carlier C, de Grazia J, Harrison KL, Johnston KP, Randolph TW, Bright FV (1997) Water core within perfluoropolyether-based microemulsions formed in supercritical carbon dioxide. *J Phys Chem* 101:6707–6714
39. Niemeyer ED, Bright FV (1998) The pH within PFPE reverse micelles formed in supercritical CO<sub>2</sub>. *J Phys Chem B* 102:1474–1478
40. Holmes JD, Ziegler KJ, Audriani M, Lee CT Jr, Bhargava PA, Steytler DC, Johnston KP (1999) Buffering the aqueous phase pH in water-in-CO<sub>2</sub> microemulsions. *J Phys Chem B* 103:5703–5711
41. Clarke MJ, Harrison KL, Johnston KP, Howdle SM (1997) Water in supercritical carbon dioxide microemulsions: spectroscopic investigation of a new environment for aqueous inorganic chemistry. *J Am Chem Soc* 119:6399–6406
42. Jacobson GB, Lee CT Jr, Johnston KP (1999) Organic synthesis in water carbon dioxide microemulsions. *J Org Chem* 64:1201–1206
43. Jacobson GB, Lee CT Jr, da Rocha RP, Johnston K P (1999) Organic synthesis in water carbon dioxide emulsions. *J Org Chem* 64:1207–1210
44. Holmes JD, Bhargava PA, Krogel BA, Johnston KP (1999) Synthesis of cadmium sulfide Q particles in water-in-CO<sub>2</sub> microemulsions. *Langmuir* 15:6613–6615
45. Holmes JD, Steytler DC, Rees GD, Robinson BH (1998) Bioconversions in a water-in-CO<sub>2</sub> microemulsion. *Langmuir* 14:6371–6376
46. Kane MA, Baker GA, Pandey, S, Bright FV (2000) Performance of cholesterol oxidase sequestered within reverse micelles formed in supercritical carbon dioxide. *Langmuir* (in press)
47. Cooper AJ, DeSimone JM (1996) Polymer synthesis and characterization in liquid/supercritical carbon dioxide. *Cur Opin Solid State Mater Sci* 1:761–768
48. Kendall JL, Canelas DA, Young JL, DeSimone JM (1999) Polymerizations in supercritical carbon dioxide. *Chem Rev* 99:543–563
49. Melnichenko YB, Kiran E, Wignall GD, Heath KD, Salaniwal S, Cochran HD, Stamm M (1999) Pressure- and temperature-induced transitions in solutions of poly(dimethylsiloxane) in supercritical carbon dioxide. *Macromolecules* 32:5344–5347
50. Gromov DG, de Pablo JJ (1998) Phase behavior of polymer-solvent mixtures. *Fluid Phase Equil* 151:657–665
51. Gromov DG, de Pablo JJ, Luna-Barcanas G, Sanchez IC, Johnston KP (1998) Simulation of phase equilibria for polymer-supercritical solvent mixtures. *J Chem Phys* 108:4647–4653



52. Luna-Barcenas G, Meredith JC, Sanchez IC, Johnston KP, Gromov DG, de Pablo JJ (1997) Relationship between polymer chain conformation and phase boundaries in a supercritical fluid. *J Chem Phys* 107:10,782–10,792
53. Luna-Barcenas G, Gromov DG, Meredith JC, Sanchez IC, dePablo JJ, Johnston KP (1997) Polymer chain collapse near the lower critical solution temperature. *Chem Phys Lett* 278:302–306
54. Gregg CJ (1994) PhD Thesis, Lehigh University and references cited therein
55. Poliakov M, George MW, Howdle SM (1999) Proceeding of the 6th meeting on supercritical fluids: Chemistry and Materials, Nottingham, UK
56. Ikushima Y, Saito N, Hatakeda K, Sato O (1996) Promotion of a lipase-catalyzed esterification in supercritical carbon dioxide in near-critical region. *Chem Eng Sci* 51:2817–2822
57. Ikushima Y, Saito N, Arai M, Blanch HW (1995) Activation of a lipase triggered by interactions with supercritical carbon dioxide in the near-critical region. *J Phys Chem* 99: 8941–8944

New Trends in Fluorescence Spectroscopy  
Applications to Chemical and Life Sciences

Valeur, B.; Brochon, J.-C. (Eds.)

2001, XXV, 490 p., Hardcover

ISBN: 978-3-540-67779-6